Elastic stresses can form metamorphic fabrics

James Gilgannon[1], Damien Freitas[1], Roberto Emanuele Rizzo[1,2], John Wheeler[3], Ian B Butler[1], Sohan Seth[1], Federica Marone[4], Christian M Schlepütz[4], Gina McGill[1], Ian Watt[1], Oliver Plümper[5], Lisa Eberhard[5], Hamed Amiri[5], Alireza Chogani[5], Florian Fusseis[1,6]

[1]School of Geosciences, The University of Edinburgh, The King's Buildings, Edinburgh EH9 3FE, UK

[2]Department of Earth Sciences, University of Florence, Via La Pira 4, 50121, Florence, IT

[3]Department of Earth, Ocean and Ecological Sciences, University of Liverpool, 4 Brownlow Street, Liverpool L69 3GP, UK

[4]Swiss Light Source, Paul Scherrer Institut, Forschungsstrasse 111, 5232 Villigen PSI, CH

[5]Department of Earth Sciences, Utrecht University, Budapestlaan 4, 3584CD Utrecht, NL

[6]Applied Structural Geology, RWTH-Aachen University, Lochnerstrasse 4-20, 52064 Aachen, DE

ABSTRACT

Detailing the relationship between stress and reactions in metamorphic rocks has been controversial and much of the debate has centred on theory. Here we add to this discussion and make a major advance by showing in time-resolved synchrotron microtomography experiments that a reacting and deforming sample experiencing an elastic differential stress produces a fabric orthogonal to the largest principal stress. This fabric forms very early in the reaction and can be shown to be unrelated to strain. The consequences of this are significant because a non-hydrostatic stress state is a very common geological occurrence. Our data provide the basis for new interpretations of the classical, and enigmatic, serpentine fabrics of Val Malenco and Cerro

del Almirez, where we relate the reported fabrics to transient, and cyclical, differential stresses from intrusion and the earthquake cycle.

INTRODUCTION

Many naturally metamorphosed rocks have mineral fabrics that define structural elements such as foliations and lineations. It is often unclear what the relative contributions of metamorphism and deformation are in the production of these fabrics. This is a fundamental question because it drives at the heart of the role of stress in metamorphism.

There are two states of stress that are of interest to the tectono-metamorphic community: one where all principal stresses are equal (hydro or lithostatic pressure) and another where at least one of the principal stresses is larger than the others (differential stress, σ_{diff}). Pressure has been shown experimentally to affect mineral stability and this fits well with our understanding of equilibrium thermodynamic predictions of metamorphic reactions (e.g. Powell and Holland 2010; Lanari and Duesterhoeft, 2019). It is also well established that metamorphic fabric development can be controlled by σ_{diff} through pressure solution (e.g. Beach, 1979; Ishii, 1988; Wheeler, 1991; Gratier et al., 2013). In this sense, fabric development has been viewed in the context of accumulated irreversible strain, both volumetric or shear, during or after a metamorphic reaction (e.g. March, 1932; Ramsay and Graham, 1970; Sintubin, 1994). However, there exist theoretical predictions of fabric development from elastic deformation (Kamb, 1959), results of anisotropy during reaction and elastic deformation (Schrank et al. 2021) and natural examples of fabrics away from deformed regions (e.g. Clément et al., 2019). These run contrary

to the expectations of how fabrics form and invites experiments that test whether an elastic σ_{diff} can directly influence a metamorphic reaction to form a fabric.

To investigate the relationship between stress, metamorphism and fabric development, we dehydrated gypsum in a series of experiments with different elastic stress states while documenting their progress with time-resolved (4D) synchrotron microtomography (μCT). Our results provide evidence for how an elastic stress field imposed during a metamorphic reaction can determine the mineral fabric of a transformation.

METHODS

We dehydrated cylindrical samples of Volterra Alabaster (gypsum, $CaSO_4 \cdot 2H_2O$) inside our X-ray transparent triaxial Mjölnir rig (Butler et al., 2020; Marti et al. 2021). The rig has been modified to have pore fluid pressure control via an independent fluid channel (fig. S1). The 4D μCT data were acquired at the TOMCAT beamline of the Swiss Light Source with one hydrostatic experiment imaged on the University of Edinburgh's (UoE) inhouse μCT system. At the conditions of our experiments gypsum dehydrates to produce bassanite ($CaSO_4 \cdot 0.5H_2O$) and water. For a constant temperature and pressure, in two main suites of constant pore fluid pressure, we varied σ_{diff} to capture its effect (table S1). Elasticity was demonstrated in experiments offline at UoE (fig. S8). The results of these experiments were then compared to a simple strain model.

Details of the apparatus, data acquisition, conditions, segmentation and model are found in the supplemental material.

RESULTS

Reaction microstructure

In all experiments the gypsum reacts to produce bassanite needles (figs. 1 and 2) with porous "moats" surrounding the needles (fig. 1). These moats never fully envelope bassanite and contact points exist between reactants and products. The reaction occurs fairly uniformly through the samples and there is no evidence of irreversible compaction of pores (fig. 3a). This is supported by an observation of the reversibility of axial strain accumulated (fig. S8). Some experiments show nucleation and growth along the central axis of the samples, related to a more efficient drainage near the pore fluid pressure outlets (fig. S1). The most notable result is that the orientation of bassanite crystals systematically changes with the imposed stress field (figs. 1 and 2). When all of the principal stresses are equal, or very close to equal, bassanite needles grow in many different orientations (fig. 1). In contrast, when σ_{diff} is increased, bassanite develops orientations perpendicular to the largest principal stress (figs. 1 and 2).

Orientation analysis of bassanite

Our 4D μCT data shows that for reaction extents of <30% and axial strains of <0.3% bassanite needles show preferred orientations (fig. 3b). Once established, the orientations do not change and are observed in post-mortem analyses. To a first approximation the alignments reflect the radial symmetry of the imposed stress (fig. 2) but there are some “symmetry-breaking” features (fig. 3b). When the largest stress is applied axially the needles develop girdles in the XY plane, with one sample’s girdle also containing a maximum (symmetry breaking). The development of a fabric early in the reaction cannot be attributed to the starting material because it is seen in both VA_s_1 and VA_A, a sample pair that were cored perpendicularly to each other.

Strain cannot explain the reaction fabric

Fabric formation from the rotation of minerals during deformation requires larger compaction strains than we observe in our samples (cf. Sintubin, 1994). This is demonstrated by a kinematic model for the "passive" rotation of material lines during axial compaction (fig. 4). Figure 4 shows the passive rotation of lines during a strain path in which the Z-axis is continually shortened. The initial orientations of the lines make up a uniform distribution. The kinematic model shows that axial strains in excess of 50% are required to develop a fabric in a rock where reaction products have nucleated without a preferred orientation. This is at odds with the strong fabrics observed early in the reaction at strains of <0.3% in our axially compressed experiments.

DISCUSSION

Our results show that a macroscopic elastic σ_{diff} can have a direct control on the formation of a fabric. Our fabrics cannot be explained by strain and it is the orientations and magnitudes of the imposed principal stresses that exert a primary control on reaction product geometry. When the largest principal stress is imposed radially a lineation is formed, whereas an axial principal stress produces a foliation girdle. These results are important because they reveal aspects of the complex relationship between microscale dissipation of energy during reaction and the bulk mechanical behaviour of a rock.

We are mindful that preferred orientations can be inherited from initial minerals which may be "templates" for nucleation and new growth (e.g. McNamara et al. 2012). Volterra gypsum can have a crystallographic preferred orientation (CPO) (Hildyard et al., 2009) and this will have a role in producing a fabric (Hildyard et al., 2011). In our reacted samples there are some "symmetry breaking" aspects to the fabrics that are likely to be related to inheritance. However,

the fact that we observe fabrics that develop with a clear relationship to the experimental geometry over multiple samples, including in a pair of perpendicular cores, suggests that inheritance only has a secondary effect. This is further supported by other similar results of fabrics in dehydration experiments where an elastic differential stress was applied (Schrank et al., 2023). These results raise several important questions and have far reaching implications.

Nucleation or growth?

There are several key observations that might help distinguish whether the stress field is influencing nucleation or growth during the metamorphic reaction: Bassanite crystals appear to grow with a similar habit and rate in all stress states, regardless of crystal orientation (fig. 1); crystals are thinner at higher σ_{diff} (fig. 1); there are load bearing contact points between gypsum and bassanite and lastly, the earliest fabrics are observed when there is no axial strain (fig. 3b) and no irreversible pore compaction recorded (fig. 3a), and all eventual strain can be recovered during unloading of an experiment (fig. S8).

We can thus establish that: 1) bassanite is anisotropic in all experiments - it is a feature of bassanite growth and not experimental conditions ; 2) crystals in unfavourable orientations with respect to the imposed stress field can grow unhampered; and 3) local stress variation contributes to material transfer through dissolution/precipitation, the proposed reaction mechanism at this temperature (cf. Bedford et al., 2017), but no irrecoverable strain (fig. S8) or sample shape changes are incurred (fig. S9). This suggests that the stress field is not affecting growth but some early step in the reaction, which we think is the nucleation step - possibly influencing the orientation of nucleation - to produce the fabric.

This is supported by recent SAXS observations from gypsum dehydration in which smaller reaction products could be resolved earlier than in our experiments. Schrank et al. (2021) found these early products to also have a bulk fabric anisotropy related to the stress field. The explanation offered in this case was that minor slip on suitably oriented gypsum (010) planes intersecting grain boundaries created sites for bassanite nucleation that when combined with the orientation of the principal stresses lead to a preferred orientation of nuclei, which is compatible with our results. This highlights the varying role of stress at different scales: a grain scale dissipation of energy but with a bulk mechanical response that is elastic.

Comparison to natural examples

Two examples of enigmatic natural metamorphic fabrics are worth comparing to our results because they occur in settings where large elastic stress perturbations will have occurred during fabric formation.

The serpentinites of Val Malenco were intruded by the Bergell composite igneous body and this triggered dehydration reactions (Clément et al., 2019; Kempf et al., 2022). This section of the high grade contact metamorphism experienced low strain (cf. Hermann et al., 1997) but hosts a foliation defined by elongated metamorphic olivine crystals (Clément et al., 2019). The CPO of the metamorphic olivine was suggested to be inherited from the unreacted antigorite, but it was also noted that the association of the CPOs was too oblique ‘to establish a clear crystallographic relationship’, that it became more variable with distance from the intrusion, that solid-state deformation could not be responsible for foliation development, nor could a link between CPOs and a regional deformational reference frame be easily established (Clément et al., 2019). With our new experimental data, one could propose that the enigmatic olivine CPO is

the result of the transient state of stress imposed by the Bergell intrusion. This notion finds support in the other experiments and field data. The dehydration at Val Malenco occurs at lower temperatures than predicted by equilibrium which can be explained by the efficiency of an elastic σ_{diff} compared to heating in triggering a reaction (Schrank et al., 2021). Additionally, evidence from contact metamorphism in the Kitakami mountains, Japan (Ishii, 1988), showed the CPO strength of newly grown chlorite and illite in cleavage planes and within aureole country rock matrix increased significantly with proximity to the intrusion (cf. fig 9 in Ishii, 1988). The spatial pattern of slaty cleavage development could not be related solely to metamorphic isograds, nor could the fabrics be explained by templating alone, with the authors ruling out strain and suggesting stress as the controlling factor.

The serpentinites of Cerro del Almirez contrast those of Val Malenco because they dehydrated in a nascent subduction zone (Jabaloy-Sánchez et al., 2015). The dehydration reaction here produces a chlorite-harzburgite that has granofels and spinifex-like microstructures (Trommsdorff et al. 1998). The reaction products, olivine and orthopyroxene, within the spinifex domains show a shape preferred orientation (SPO) and CPO in the plane perpendicular to the largest paleo-stress. Olivine within the granofels microstructure shows no CPO but has a weak layering, in the same plane as the serpentinite foliation (perpendicular to the least paleo-stress) (cf. fig. 13 in Dilissen et al., 2018). Two explanations have been offered for the bimodal texture: (1) that fast and slow drainage of fluid formed the spinifex and granofels textures respectively (Padron-Navarta et al., 2011); and (2) that spinifex olivine record crystallisation after coseismic melting (Evans and Cowan, 2012). Our results can provide an alternative explanation for the bimodal microstructure: a changing stress field may have affected the reaction fabric. Subduction

zones are known to build up and release elastic stresses during the earthquake cycle, where σ_{diff} is raised and lowered cyclically. The spinifex microstructure, forming at a high angle to the largest principal paleo-stress of the subduction interface (Dilissen et al., 2018), might reflect times of loading towards a peak σ_{diff}. The granofels microstructure, which has no olivine CPO and a weak foliation aligned with the serpentinite fabric, could record post-seismic periods. There is a switch in the orientations of the largest and least principal stresses and a reduction in σ_{diff} during this part of the cycle (cf. Hasegawa et al., 2012; Lin et al., 2013; Dielforder et al., 2015) which could allow inheritance to dominate and establish the weak SPO observed in the granofels. Thus the dehydration products found at Cerro del Almirez might evidence ongoing reaction in a tectonic setting where an oscillating non-hydrostatic stress state can determine fabric elements.

IMPLICATIONS AND CONCLUSIONS

We can conclude from our experimental results that the state of stress during a metamorphic reaction matters. There is a measurable effect of an elastic σ_{diff} on metamorphic reactions by way of fabric development. This is an important finding, because it is very common for reacting rocks to experience a σ_{diff}. Our results provide a new way to interpret many natural metamorphic fabrics and have implications for the hydraulic, mechanical and geophysical properties of reacting and deforming rocks. For example, a girdle or lineation reaction fabric will influence the permeability and seismic anisotropy differently. A lineation of product phases may channel fluid more effectively than a girdle fabric and these two fabrics will produce opposite transverse seismic wave anisotropy (e.g. Ji et al., 2015). This means that the hydrodynamics of a dehydration reaction might be uniquely determined by the geometry of the stress field and any

resulting irreversible compaction. Our results also have implications for the interpretations of strain from metamorphic fabrics. It is well documented that fabrics can form because of irreversible mechanical creep and criteria should be developed to distinguish these from earlier fabrics forming when a rock is still purely elastic. This will be difficult in highly deformed rocks because there are inevitable cycles of overprinting of microstructural elements. However as most metamorphic rocks have not suffered extreme strain localisation there will be many examples in the field where criteria can be developed to discriminate between stress and strain related fabrics.

ACKNOWLEDGMENTS

This research was funded through NERC standard grant NE/T001615/1. The Paul Scherrer Institut, Villigen, Switzerland, is acknowledged for provision of synchrotron radiation beamtime at the TOMCAT beamline X02DA of the SLS. Christoph Schrank, Stefan Schmalholz and two anonymous reviewers are thanked for their helpful comments.

REFERENCES CITED

Beach, A., 1979, Pressure solution as a metamorphic process in deformed terrigenous sedimentary rocks: Lithos, v. 12, no. 1, p.51–58, doi:10.1016/0024-4937(79)90062-8.

Bedford, J., Fusseis, F., Leclère, H., Wheeler, J., and Faulkner, D., 2017, A 4D view on the evolution of metamorphic dehydration reactions: Scientific Reports, v. 7, doi:10.1038/s41598-017-07160-5.

Butler, I.B., Fusseis, F., Cartwright-Taylor, A., and Flynn, M., 2020, Mjölnir: a miniature triaxial rock deformation apparatus for 4D synchrotron X-ray microtomography: Journal of synchrotron radiation, v. 27, p. 1681–1687, doi:10.1107/S160057752001173X.

Clément, M., Padrón-Navarta, J.A., and Tommasi, A., 2019, Interplay between Fluid Extraction

Mechanisms and Antigorite Dehydration Reactions (Val Malenco, Italian Alps): Journal of Petrology, v. 60, no. 10, p. 1935–1962, doi: 10.1093/petrology/egz058.

Dilissen, N., Hidas, K., Garrido, C.J., Wolf-Achim, K., Sánchez-Vizcaíno, V.L., and Padrón-Navarta, J.A., 2018, Textural evolution during high-pressure dehydration of serpentinite to peridotite and its relation to stress orientations and kinematics of subducting slabs: Insights from the Almirez ultramafic massif: Lithos, v. 320-321, p. 470–489, doi:10.1016/j.lithos.2018.09.033.

Dielforder, A., Vollstaedt, H., Vennemann, T., Berger, A., and Herwegh, M., 2015, Linking megathrust earthquakes to brittle deformation in a fossil accretionary complex: Nature Communications, v. 6, doi:10.1038/ncomms8504.

Evans, B.W., and Cowan, D.S., 2012, A MELT ORIGIN FOR SPINIFEX-TEXTURED METAPERIDOTITE IN THE CERRO DEL ALMIREZ MASSIF, SOUTHERN SPAIN: American Journal of Science, v. 312, p. 967–993, doi:10.2475/09.2012.01.

Gratier, J-P., Dysthe, D.K., and Renard, F., 2013, Chapter 2 - The Role of Pressure Solution Creep in the Ductility of the Earth's Upper Crust, in Dmowska, D., ed., Advances in Geophysics, v. 54, p.47–179, doi:10.1016/B978-0-12-380940-7.00002-0.

Hasegawa, A., Yoshida, K., Okada, T., Iinuma, T., and Ito, Y., 2012, Change in stress field after the 2011 great Tohoku-Oki earthquake: Earth and Planetary Science Letters, v. 355-356, p. 231–243, doi:10.1016/j.epsl.2012.08.042.

Hermann, J., Müntener, O., Trommsdorff, V., Hansmann, W., and Piccardo, G.B., 1997, Fossil crust-to-mantle transition, Val Malenco (Italian Alps): Journal of Geophysical Research, v. 102, no. B9, p. 20123–20132, doi:10.1029/97JB01510.

Hildyard, R.C, Prior, D.J., Mariani, E., Faulkner, D.R., 2009, Crystallographic preferred orientation (CPO) of gypsum measured by electron backscatter diffraction (EBSD): Journal of Microscopy, v. 236, p. 159–164, doi:10.1111/j.1365-2818.2009.03292.x.

Hildyard, R.C, Llana-Fúnez, S., Wheeler, J., Faulkner, D.R., Prior, D.J., 2011, Electron Backscatter Diffraction (EBSD) Analysis of Bassanite Transformation Textures and Crystal Structure Produced from Experimentally Deformed and Dehydrated Gypsum: Journal of Petrology, v. 52, no. 5, p. 839–856, doi:10.1093/petrology/egr004.

Ishii, K., 1988, Grain growth and re-orientation of phyllosilicate minerals during the development of slaty cleavage in the South Kitakami Mountains, northeast Japan: Journal of Structural Geology, v. 10, no. 2, p. 145–154, doi:10.1016/0191-8141(88)90112-5.

Jabaloy-Sánchez, A., Gómez-Pugnaire, M.T., Padrón-Navarta, J.A., Sánchez-Vizcaíno, V.L., and Garrido, C.J., 2015, Subduction- and exhumation-related structures preserved in metaserpentinites and associated metasediments from the Nevado–Filábride Complex (Betic Cordillera, SE Spain): Tectonophysics, v. 644-645, p. 40–57, doi: 10.1016/ j.tecto.2014.12.022.

Ji, S., Shao, T., Michibayashi, K., Oya, S., Satsukawa, T., Wang, Q., Zhao, W., and Salisbury, M.H., 2015, Magnitude and symmetry of seismic anisotropy in mica- and amphibole-bearing metamorphic rocks and implications for tectonic interpretation of seismic data from the southeast Tibetan Plateau: Journal of Geophysical Research: Solid Earth, v. 120, p. 6404–6430, doi:10.1002/2015JB012209.

Kamb, W.B. (1959), Theory of preferred crystal orientation developed by crystallization under stress: The Journal of Geology, v.67, no.2, p. 153–170, doi:10.1086/626571.

Kempf, E.D., Hermann, J., and Connolly, J.A.D., 2022, Serpentinite dehydration at low pressures: Swiss Journal of Geosciences, v. 115, doi:10.1186/s00015-022-00415-y.

Lanari, P., and Duesterhoeft, E., 2019, Modeling Metamorphic Rocks Using Equilibrium Thermodynamics and Internally Consistent Databases: Past Achievements, Problems and Perspectives: Journal of Petrology, v. 60, no. 1, p. 19–56, doi:10.1093/petrology/egy105.

March, A., 1932, Mathematische Theorie der Regelung nach der Korngestah bei affiner Deformation: Zeitschrift für Kristallographie - Crystalline Materials, v. 81, no. 1-6, p. 285–297, doi:10.1524/zkri.1932.81.1.285.

Marone, F., and Stampanoni, M., 2012, Regridding reconstruction algorithm for real time tomographic imaging: Journal of synchrotron radiation, v. 19, p. 1029–1037, doi: 10.1107/S0909049512032864.

Marti, S., Fusseis, F., Butler, I.B., Christian Schlepütz, C., Marone, F., Gilgannon, J., Kilian, R., and Yang, Y., 2021, Time-resolved grain-scale 3D imaging of hydrofracturing in halite layers induced by gypsum dehydration and pore fluid pressure buildup: Earth and Planetary Science Letters, v. 554, doi:10.1016/j.epsl.2020.116679.

McConnell, J.D.C., Astill, D.M., and Hall, P.L., 1987, The pressure dependence of the dehydration of gypsum to bassanite: Mineralogical Magazine, v. 51, 453–457, doi: 10.1180/minmag.1987.051.361.12.

McNamara, D.D., Wheeler, J., Pearce, M., Prior D.J., 2012, Fabrics produced mimetically during static metamorphism in retrogressed eclogites from the Zermatt-Saas zone, Western Italian Alps: Journal of Structural Geology, v. 44, p. 167–178, doi:10.1016/ j.jsg.2012.08.006.

Padrón-Navarta, J.A., Sánchez-Vizcaíno, V.L., Garrido, C.J., and Gómez-Pugnaire, M.T., 2011, Metamorphic Record of High-pressure Dehydration of Antigorite Serpentinite to Chlorite Harzburgite in a Subduction Setting (Cerro del Almirez, Nevado-Filábride Complex, Southern Spain): Journal of Petrology, v. 52, no. 10, p. 2047–2078, doi:10.1093/petrology/egr039.

Powell, R., and Holland, T., 2010, Using Equilibrium Thermodynamics to Understand Metamorphism and Metamorphic Rocks: Elements, v. 6, p. 309–314, doi:10.2113/gselements.6.5.309.

Ramsay, J.G., 1967, Folding and fracturing of rocks. The Blackburn Press.

Ramsay, J.G., and Graham, R.H., 1970, Strain variation in shear belts: Canadian Journal of Earth Sciences, v. 7, no. 3, p. 786–813, doi:10.1139/e70-078.

Rizzo, R.E., Freitas, D., Gilgannon, J., Seth, S., Butler, I.B., McGill, G., and Fusseis, F., 2023, Using Internal Standards in Time-resolved X-ray Micro-computed Tomography to Quantify Grain-scale Developments in Solid State Mineral Reactions: EGUsphere, p. 1–27, doi:10.5194/egusphere-2023-1819.

Schrank, C.E., Blach, T., Ji, Y., Vu, P., Wang, X., Jones, M., Kirby, N., Seibt, S., and Regenauer-Lieb, K., 2023, Stress sensitivity of gypsum dehydration kinetics at constant uniaxial stress under dry conditions: : EGU General Assembly 2023, EGU23-7120, doi:10.5194/egusphere-egu23-9856.

Schrank, C.E., Gaede, O., Blach, T., Gioseffi, K., Mudie, S., Kirby, N., Regenauer-Lieb, K., and Radlinski, A.P., 2021, Fast in-situ X-ray scattering reveals stress sensitivity of gypsum dehydration kinetics: Communications Materials, v. 2, doi:10.1038/s43246-021-00156-9.

Sintubin, M., 1994, Clay fabrics in relation to the burial history of shales: Sedimentology, v. 41, p. 1161–1169, doi:10.1111/j.1365-3091.1994.tb01447.x.

Trommsdorff, V., Sánchez-Vizcaíno, V.L., Gómez-Pugnaire, M.T., and Müntener, O., 1998, High pressure breakdown of antigorite to spinifex-textured olivine and orthopyroxene, SE Spain: Contributions to Mineralogy and Petrology, v. 132, p. 139–148, doi:10.1007/s004100050412.

Van Driessche, A.E.S., Stawski, T.M., Benning, L.G., and Kellermeier, M., 2017, Calcium Sulfate Precipitation Throughout Its Phase Diagram: New Perspectives on Mineral Nucleation and Growth: From Solution Precursors to Solid Materials, doi: 10.1007/978-3-319-45669-0 12.

Wheeler, J., 1991, A view of texture dynamics: Terra Nova, v. 3, no. 2, p. 123–136, doi:10.1111/j.1365-3121.1991.tb00864.x.

FIGURES

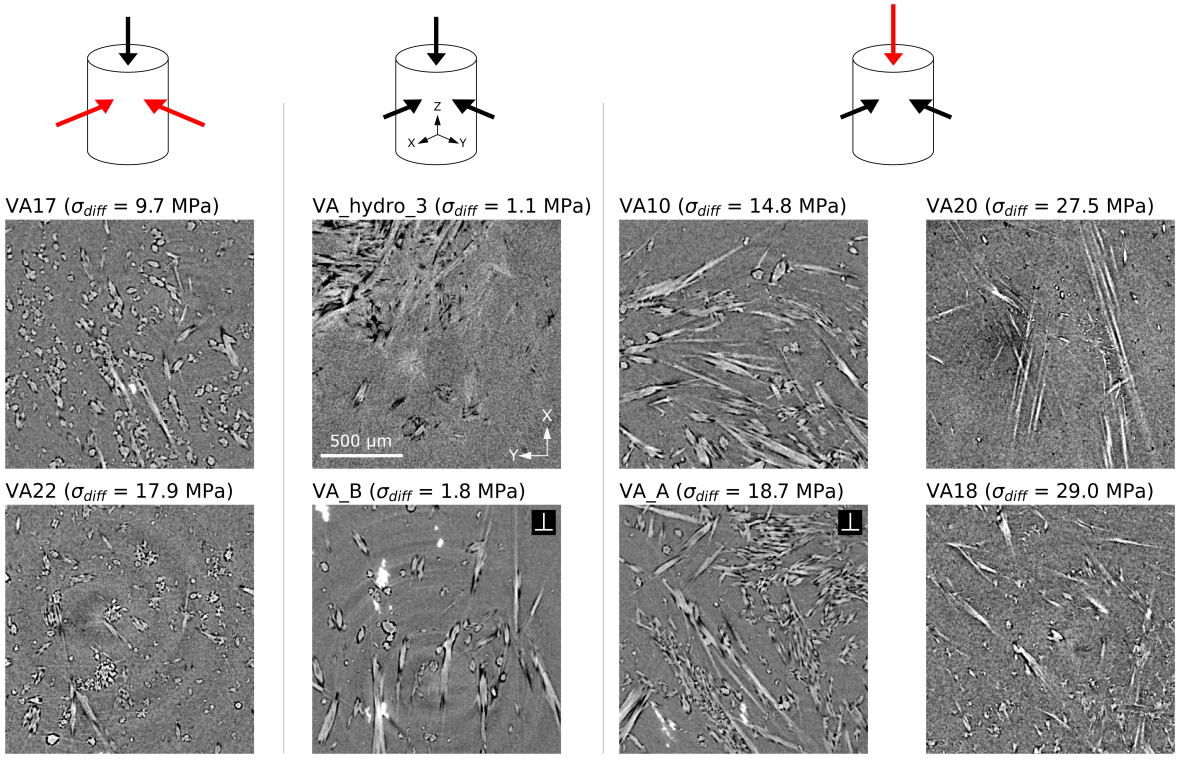

Figure 1. Microstructures from three stress states (gypsum = dark grey; bassanite = light grey; pores = black; celestite = white; σ_{diff} error = ±0.9 MPa). Hydrostatic experiments have bassanite needles with a variety of orientations. A σ_{diff} produces needles with long axes perpendicular to the largest principal stress (red arrows). ⊥ = perpendicularly cored sample.

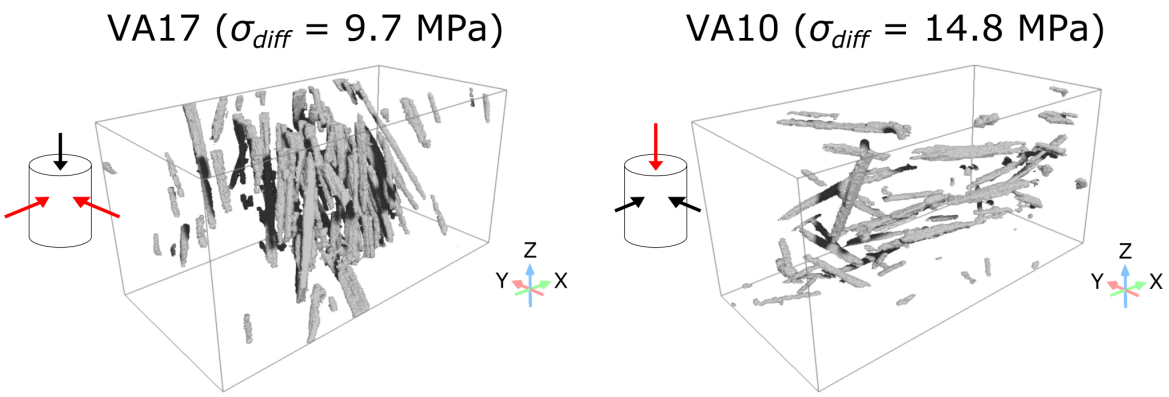

Figure 2. 3D rendering of bassanite in different experiments (VA17 reaction extent = 30%; VA10 reaction extent = 0.7%). Box heights are 500 µm.

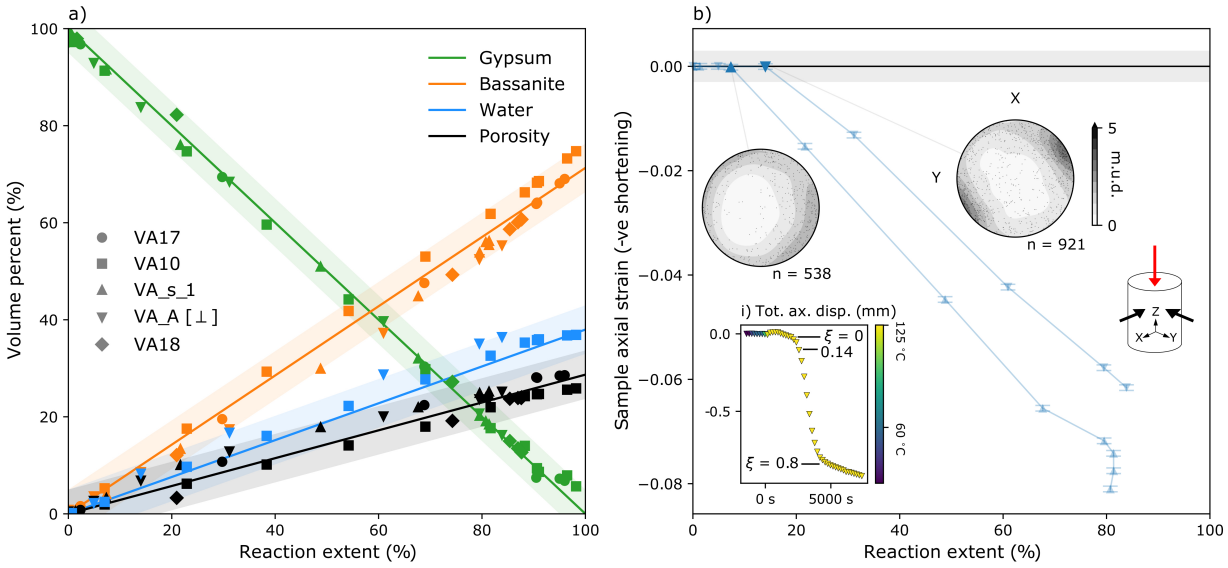

Figure 3. Reaction evolution in four samples. a) Segmented data compared to the theoretical curves for phases with no compaction (coloured line) and 5% accuracy envelopes (shaded areas). b) Bassanite orientations (lower hem., equal area; m.u.d. = multiples of uniform distribution) contextualised in strain. Grey region is ±0.003, the strain resolution, while the error bars are the uncertainty. ξ = reaction extent.

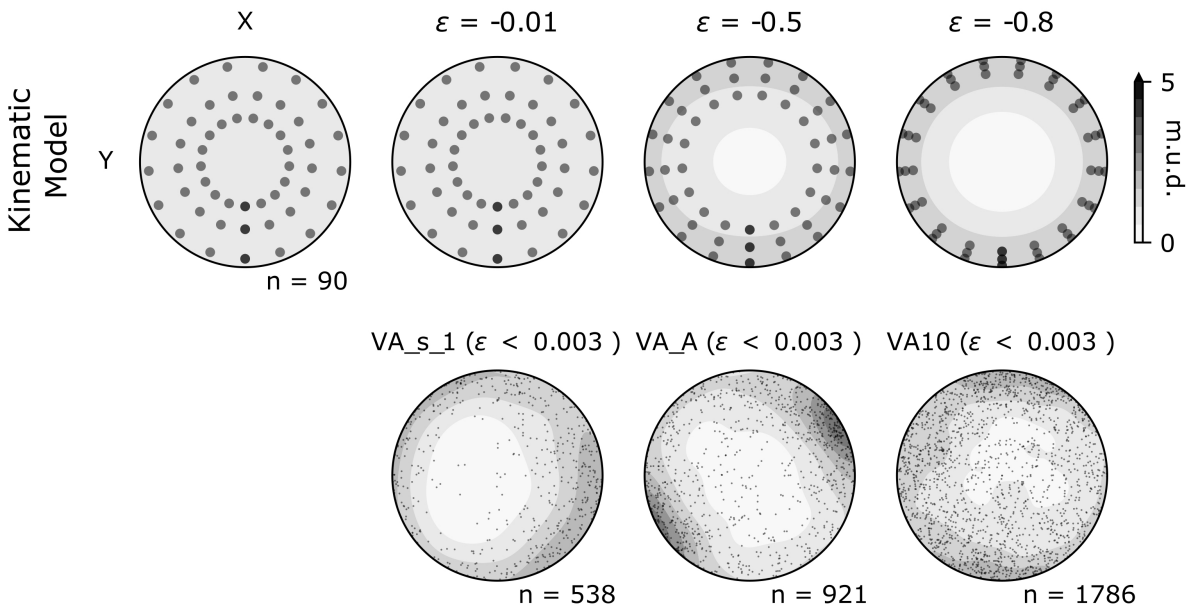

Figure 4. Comparison of a kinematic model of line rotations with axial strain (ε) and experimental observations.